School of Mechanical Engineering
The University of Western Australia

Battery Restraint System Design And Performance Evaluation for Renewable Energy Vehicle Project

Chun Shing Ip

November 2008

Supervisor: Dr Kamy Cheng

Abstract

In Australia, the current transport energy use is extremely inefficient due to heavy dependence on personal transport systems. Although public transport is available, it is considered slow and impractical compared with personal transport. To combat these issues, the Renewable Energy Vehicle of the University of Western Australia is created in effort to rises the awareness of renewable energy within the University and wider community.

In this project, the battery restraint system must be designed and built by considering the constraints imposed and adhering to the relevant codes and regulations. To achieve these, the prototype of the potential design was created with the aid of SolidWorks and subsequently analysis under specific condition was conducted through the use of ANSYS Workbench.

This project also evaluated the propulsion power requirement by determining the resisting forces acting on the vehicle. Nevertheless investigation into the effect of variations in ride height and weight distribution on the handling behaviour was performed using a standard vehicle as datum.

The procedures established in this study will provide a basis for future battery restraint system design, as well as future performance evaluation.

Letter of Transmittal

Chun Shing Ip
51 Colombo Street
Victoria Park, 6100

3 November 2008

Associate Professor Carolyn Oldham
Dean
Faculty of Engineering, Computing and Mathematics
University of Western Australia
35 Stirling Highway
Crawley, WA 6009

Dear Associate Professor Oldham,

I am pleased to present this thesis, entitled "Battery Restraint System Design and Performance Evaluation for the Renewable Energy Vehicle Project" as part of the requirement for the degree of Bachelor of Engineering.

Yours sincerely,

Chun Shing Ip
10547880

Acknowledgements

The successful completion of this project would not have been possible without assistance from the following people, who I would like to sincerely thank,

To Dr Kamy Cheng, for his unlimited enthusiasm, unique open-mindedness and dedicated supervision.

To A/Professor Braunl Thomas, for all your advice on the battery restraint system design

To Ken Fogden, Brian Cowling, Neil Shearn and George Voyt of the Electrical Engineering workshop, for their time and effort during the manufacture of the battery compartment frame.

To the UWA REV team, for the opportunity to take part in this innovative project.

To Dyizen Tan and Winston Ma, for their help in the performance evaluations

To my Parents, May Ip, for giving me the support and independence required to take on such a task.

Table of Contents

Table of Figures

List of Tables

NOMENCLATURE

v	Relative wind speed
A_f	Equivalent frontal area
C_d	Drag coefficient
C_r	Rolling resistance coefficient
F_d	Aerodynamic drag force
F_h	Gravitational force
F_r	Rolling resistance force
F_{TR}	Tractive force
F_y	Force in y-direction
L_i	Distance
M_A	Moment at Point A
R_A	Reaction force at Point A
R_B	Reaction force at Point B
W	Vehicle weight
$W_{batteries}$	Weight of batteries including the battery compartment
W_{engine}	Weight
$W_{fuel\ tank}$	Weight of fuel tank (including 45 L of gasoline)
η	Electric motor efficiency
ρ	Density of the fluid

Φ	Angle of inclination

1 Introduction

1.1 Background

Australian Bureau of Statistics found that there were over 14 million motor vehicles that are registered as using petrol as fuel with the average distance travelled annually of 14, 300 kilometres in Australia in 2007. Although public transport is available, it is considered slow and impractical compared with personal transport. As a result, the current heavy dependence of personal transport systems is responsible for 13% of Australia's greenhouse gas emissions and the current transport energy use is extremely inefficient. Moreover, fossil fuels are finite resources and fast running out. In recent years, the price of fossil fuels has risen sharply. Hence, it is crucial to develop a renewable energy technology. Vehicles supplied by renewable energy sources present the prospect of energy utilisation with minimum impact on the environment, particularly in relation to greenhouse gas emission. More importantly, renewable energy source is a sustainable energy source which can be relied on for the long-term future.

The UWA Renewable Energy Vehicle project first started in July 2004 was inspired by Tamagwa University's Solar Car Project, which successfully drove a hybrid solar and fuel cell powered vehicle across Australia, as well as UWA's own Motorsport team and robotics projects (Mathew 2008).

In 2008, REV team with 14 students from the School of Electrical, Electronic and Computer Engineering and the School of Mechanical Engineering aims to revolutionise personal transport by building vehicles that produce no pollution, powered by electricity from any point and viable to both the commercial and performance markets, by using existing production cars and converting them to use electricity as its sole source of propulsion. The aim of this project is to work with a project team to build a four-wheel, five-seater commuter electric car and also a performance electric car, with particular interest in the battery restraint system, aerodynamic analysis and the handling behaviour evaluation.

The ideal outcome of this project will see that this year the Hyundai Getz have sustained performance. Most of this project's work will become evident once the designs are manufactured and is able to test run the car.

1.2 Project objective

The project objectives for the power and drag analysis, design of the battery restraint system and the handling behaviour evaluation are outlined below:

- Conduct literature survey to investigate the effect of variation in ride height and weight distribution on vehicle handling behaviour and to research the existing battery restraint system design in other projects
- Evaluate the propulsion power required for the electric vehicle
- Identify the design constraints that will restrict the potential designs for the battery constraint system
- The battery restraint system must be fully compliant with the relevant codes and regulations.
- Create the prototype geometry of the potential designs with the aid of computer aided drafting (CAD) software
- Investigate the reliability of the potential designs for the battery restraint system using finite element analysis software
- Investigate the handling behaviour of the converted Hyundai Getz using a standard Hyundai Getz as datum

2 Literature Survey

2.1 Chapter Overview

This chapter discusses the concept designs of the battery restraint system that are commonly used in electric cars. This chapter also discusses ride height in detail and how the front-to-rear weight distribution can affects the ride height.

2.2 Battery Restraint System

2.2.1 Battery Location

To determine the location of the batteries, the obvious considerations are available space, weight distribution and current path. The most ideal arrangement would be to have all the batteries in a single block. In a typical passenger car, however, the batteries are always split between the front and rear of the car due to limited space.

2.2.2 Battery Rack

Battery rack is used to secure the batteries in place, even during a collision or rollover. Brown (1993) recommends that minimum dimensions of the battery rack should be no less than 4.8 mm thick and 38.1 mm wide using steel angle stock. It is also proposed that reinforcing straps at bottom are required if the rack is large (Brown 1993).

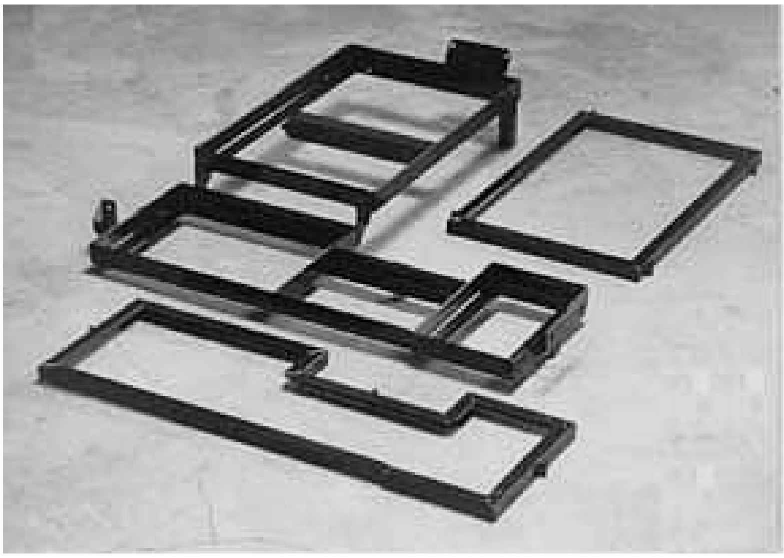

Figure 2.1: Battery rack and hold-down frames (Brown 1993)

In addition, bars or rigid straps are usually bolted into place across the tops for battery box while angle stock frame can be used for batteries that are not enclosed in boxes. If the bars or straps are made of metal, they must be well placed in order to prevent short-circuit across two terminals. (Brown 1993)

2.2.3 Ventilation

It is important that batteries enclosed in boxes to be ventilated, especially boxes that are located in the passenger compartment. The reason for this is that hydrogen, which may be produced during battery charging and discharging, could explode. Ventilation can be achieved by installing a non-arcing fan. (Brown 1993)

2.3 Ride Height

Ride height is the distance between a specific point on the chassis, suspension or body and the ground as shown in Figure 2.2. Change in ride height may affect the suspension geometries, for example, camber, caster and toe.

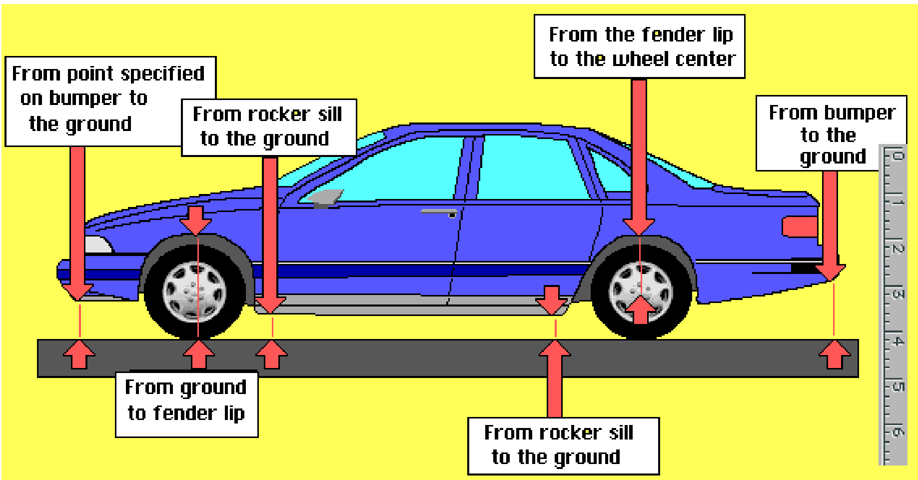

Figure 2.2: Method of measuring ride height (Carley 2005)

When converting a car to electricity, the original front-to-rear weight distribution is often changed depending on the modification. If a car is heavy on one end and light on the other, the spring effect will cause the light end to sit higher than before. As a result, the factory standard front and rear ride heights will be altered (Brown 1993). It is crucial to measure the front and rear ride heights and compare the results with the factory specification when the conversion is completed. If the ride height is found to be lost or gained, spring adjustment or replacement should be performed.

Alteration to the factory specified ride height may possibly have an adverse effect on steering ability depending on the amount of change. The aim of the headlights may also be affected as a result of changes in ride height, which in turn affects night-time driving safety (Carley 2005).

2.3.1 Effect of Variation in Ride Height

For all vehicles, Carley (2005) stated that variations in ride height could lead to several problems relating to handling, practicality and also attitude change. First, the chassis and under-body of the car may be damaged and may scrape against the road when the vehicle is being driven on roads that are not level. In addition, the steering geometry of the front suspension may possibly be upset if the rear ride height is raised or lowered. The adverse effects depend on the amount of changes (Brown 1993). Moreover, the original aim of the headlamp could be altered when raising or lowering the front ride height. The change in the aiming of the headlamp may affect the night-time driving safety (Carley 2005).

2.4 Effect of Front-to-Rear Weight Distribution

Front-to rear weight distribution is the distribution of weight at the front and rear axles of the vehicle. It is one of the critical factors that govern the vehicle handling, particularly during cornering. Uneven front-to-rear weight distribution is considered to be the most significant contributor to oversteer or understeer (Bastow, Howard & Whitehead 2004). Understeer is defined as the tendency for a vehicle to travel in a straight while oversteering is as the tendency for a vehicle to spin. If a vehicle is heavier at the front, the centre of gravity is located near the front and thus understeer is introduced. On the contrary, rear-heavy vehicle has the centre of gravity located near the rear end and thus oversteer is introduced.

It is very common for the vehicle manufacturer to configure production cars to have a slight understeer by default because it provides inherent stability (Wikipedia (a) 2008). An understeering car tends to travel in a straight line, whereas an oversteering car tends to spin during cornering. Bastow, Howard & Whitehead (2004) proposed that the oversteering car has an associated critical speed beyond which the car will turn violently in response to the slightest steering input or even disturbance.

In understanding the handling stability of a car, the position of the neutral steer point (NSP) in relation to the positions of the centre of gravity (CG) and the aerodynamic centre of the pressure (COP) play as important roles (Bastow, Howard & Whitehead 2004). The NSP can be defined as the point at which the laterally applied force could cause a vehicle to move sideways without yawing while the centre of pressure can defined as the point on the car at which the sum total of the aerodynamic pressure acts. For handling stability during cornering, the NSP must be located behind the CG as illustrated in Figure 2.3. Consider the car depicted in Figure 2.3 is describing a left turn. The tyre forces acting at the NCP is toward the left, whereas the inertia forces acting at the CG is toward the right. As a result of these two forces, the car tends to turn to the right (Bastow, Howard & Whitehead 2004). This means that the car is tending to make it go in a straight line. If the car is subjected to side winds,

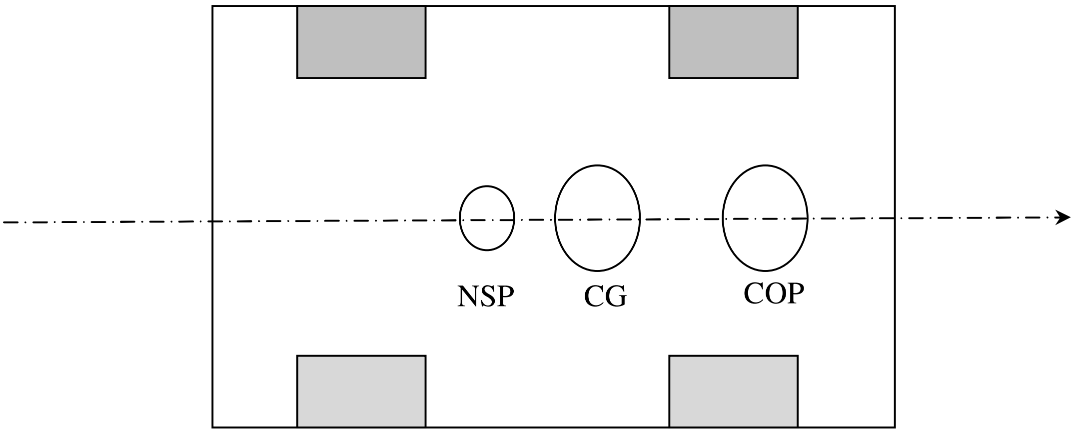

Figure 2.3: Relative positions of the centre of gravity (CG), the neutral steer point (NSP), and the centre of pressure (COP)

In a front-heavy car, the CG is typically located near the front end with the COP located ahead of it and the NSP located behind of it (Bastow, Howard & Whitehead 2004). Although the NSP is located behind the CG, it is most likely to be nearer the front than the back. For this reason, the separation of the NSP from the COP is relatively small and as a result the yawing moment due to side wind will be relatively small. On the other hand, the COP is likely to be nearer the front with the CG located nearer the rear end for a rear-heavy car(Bastow, Howard & Whitehead 2004). Consequently, the yawing moment caused by the side wind is correspondingly large due to relatively large separation of the NSP from the COP.

Bastow, Howard & Whitehead (2004) suggested that there are two possible ways to make a rear-heavy car stable in terms of understeer. Firstly, it can be done by having larger rear tyres than front ones. In addition, the rear-heavy car could be more stable by the choice of suspension design and setting. Although the rear-heavy can be made stable, it is difficult to shift the COP in the rearward direction in order to minimise the wind-induced yawing moment.

3 Electric Vehicle Power and Drag Analysis

The fundamentals of electric vehicle design are embedded in the basic mechanics of physics, particularly in Newton's second law of motion relating force and acceleration. Newton's second law states that the acceleration of an object is proportional to the net force exerted on it. The object accelerates only if the summation of forces acting on it is non-zero. In the electric vehicle system, vehicle accelerates when forces generated by the electric motor overcome the resisting forces acting on the vehicle caused by the gravity, air and tyre resistance (Brant 1994).For this reason, the requirements of power and energy play an important role in the design of electric vehicle as the more power and energy required to overcome the resisting force the shorter range. In order to calculate the power and energy required for a vehicle, the roadway and vehicle kinetics were analysed. With the power and energy requirements defined, the range for a given energy source could then be predicted.

3.1 Road Load Force

Road load force, $F_{FL,}$ is the opposing force acting on the vehicle in an opposite direction. It is composed of the hill-climbing force, aerodynamic drag force, rolling resistance of the tyres and the gravitational force. The components of the road load force are:

3.1.1 Gravitational Force

The gravitational force varies with the slope of the roadway. The force is positive when climbing a slope and is negative when descending a downgrade roadway. When vehicle climbs up a slope, the gravitational force can be decomposed into two vectors as shown in Figure 3.1, one perpendicular to the roadway and one parallel to the roadway (Brant 1994). The gravitational force to be overcome by the vehicle moving forward is (Brant 1994)

$$F_h = W \cdot \sin\varphi \tag{3.1}$$

where $F_{gravity}$ is the gravitational force, W is the vehicle weight in newtons (N), and φ is the angle of inclination. The gravitational force exerted on the vehicle depends of the angle of inclination as sin φ varies from 0 at no incline to 1 at 90 degrees. The angle of inclination can be calculated by

$$\text{Angle of inclination, } \varphi = \text{Arctan } \frac{\text{Rise}}{\text{Run}} \tag{3.2}$$

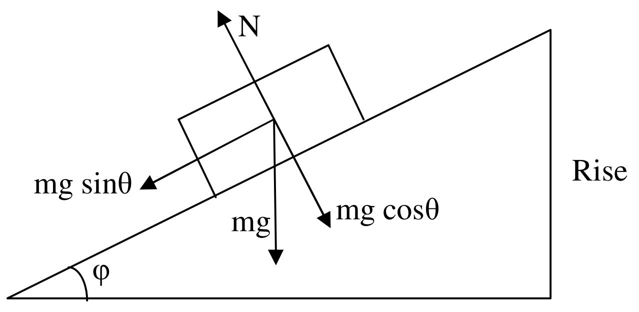

Figure 3.1: Free body diagram on an inclined plane

3.1.2 Aerodynamic Drag Force

Aerodynamic drag can be defined as the retarding force on vehicle acting in the opposition of movement. It is the result of viscous resistance and pressure distribution over the body of air working against the motion of the vehicle (Brant 1994). The force can be expressed as:

$$F_d = \frac{1}{2} \rho C_d A_f v^2 \tag{3.3}$$

where F_d is the aerodynamic drag force measured in newtons (N), ρ is the density of the fluid measured in kg/m^3, C_d is the drag coefficient (dimensionless, and typically is $0.2 < C_d < 0.4$), A_f is the equivalent frontal area of the vehicle in m^2, and v is the relative wind speed in m/s (the speed of the fluid moving past the vehicle. If the vehicle itself is moving while facing a headwind, the headwind speed has to be added to the speed of the vehicle to obtain).

3.1.3 Rolling Resistance of Tyres

The rolling resistance is the force resisting the motion when a tyre rolls on a flat surface. It is caused by the deformation of the tyre, the deformation of the surface, or both (Brant 1994). It varies with different materials of the tyre and the sort of the ground. The rolling resistance can be expressed as

$$F_r = C_r W \cos\varphi \tag{3.4}$$

where F_r is the rolling resistance force, C_r is the rolling resistance coefficient (typically is $0.01 < C_r < 0.3$ depending on the ground condition and tyre's material), W is the weight measured in newtons (N), and φ is the angle of inclination as shown in Fig 3.1 (Brant 1994). The rolling resistance force exerted on the vehicle depends of the angle of inclination as sin φ varies from 0 at no incline to 1 at 90 degrees.

3.2 Tractive Force and Tractive Power

Tractive force, F_{TR}, is the force supplied by the propulsion unit. In order to propel the vehicle forward at a desired constant velocity, the tractive force exerted must overcome the opposing road load force. Therefore, the tractive force exerted must be equal in magnitude to the road load force. The tractive force can be expressed as (Brant 1994):

$$F_{TR} = F_h + F_d + F_r \tag{3.5}$$

$$F_{TR} = W \cdot \sin\varphi + \frac{1}{2}\rho C_d A_f v^2 + C_r W \cdot \cos\varphi \tag{3.6}$$

The tractive power is the power required to propel the vehicle forward at a desired constant speed. It depends on the speed of the vehicle. The tractive power is given as:

$$\text{Power} = F_{TR} \cdot v \tag{3.7}$$

where tractive power is measured in Watts, F_{TR} is in newtons (N), v is in m/s.

3.3 Propulsion Power

Propulsion power is the power required to generate by the propulsion unit in order to propel the vehicle forward. It is always larger than the tractive power in magnitude as a result of the energy losses of the electric motor. The propulsion power depends on the motor efficiency and can be defined as:

$$\text{Propulsion Power} = \frac{\text{Power}}{\eta} \tag{3.8}$$

where η is the electric motor efficiency.

3.4 Propulsion Power Required for Hyundai Getz and Lotus Elise

Based on the equations described above, the power required from the electric motor can be calculated. The calculations of the propulsion power required for the Hyundai Getz and Lotus Elise were performed with the aid of Excel spreadsheet. For the calculation of the propulsion power required for Hyundai Getz, the technical specifications, environmental parameters and roadway conditions are as follows:

Environmental Parameters

Density of air	- 1.204 kg/m^3 at 20 ºC (Wikipedia (b) 2008)
Gravity	- 9.81 m/s^2

Roadway conditions

Headwind speed	- 0 km/h
Uphill incline (Slope)	- 0

Vehicle Parameters

Aerodynamic drag coefficient	- 0.32
Equivalent car frontal area	- 2.49 m^2 (Cartoday 2006)
Vehicle mass	- 1565 kg
Motor efficiency	- 88 %
Rolling resistance coefficient (tyre)	- 0.011 confirmed by Mr Heusden (Kumho Tire)

The propulsion power required at different speed is shown in Table 3.1. It can be seen that the propulsion power required for the Hyundai Getz is directly proportional to the speed. This was because the road load forces acting on the vehicle increases with the speed. Although the propulsion power required was evaluated, the calculation of the road range is not included in this thesis as it is beyond the author's scope.

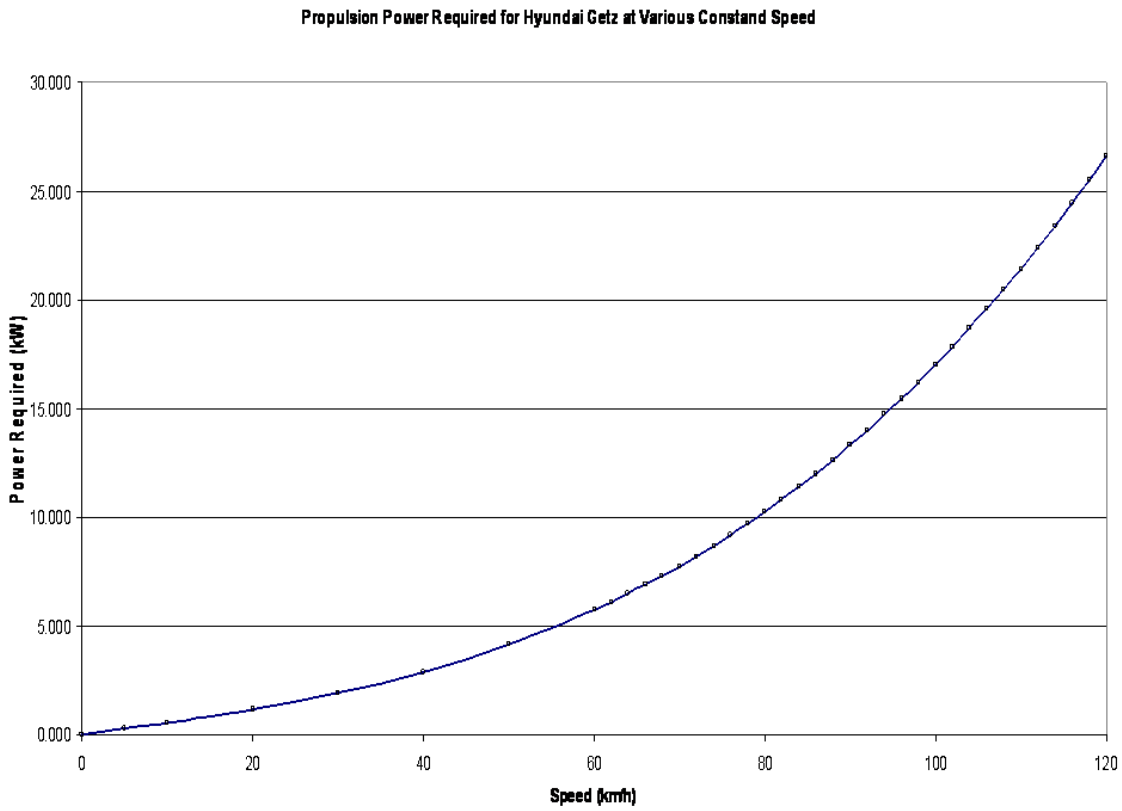

Table 3.1: Propulsion power required for the Hyundai Getz at various speed

4 Battery Restraint System Design for Hyundai Getz

4.1 Methodology

This section covers the constraints imposed on the design and provides a description of the computer modelling tools employed during the design process. It also discusses the relevant codes and regulations and framework for evaluating the success of the resulting design.

4.1.1 Constraints

Definition of the constraints is of enormous assistance in obtaining the design solution as it helps in narrowing down the range of possible solutions. There were three main sources of constraints on the design of the battery constraint system for the Hyundai Getz. These constraints were the aims of the project, battery specification and the Australian Design Rules (ADRs) and the National Code of Practice for Light Vehicle Construction and Modification (NCOP).

4.1.1.1 Aims of the REV Project

The constraints imposed by the aims of the design project are shown as follow:

- Fully compliant with the ADRs and NCOP
- Reliable
- Light weight
- Low cost
- High accessibility for battery inspection
- Corrosion resistant

4.1.1.2 Battery Specification

Forty five 3.2V Thunder Sky lithium-ion batteries (Model No. – TS-LFP90AHA) were chosen as the energy source, weighing 3.2 kg each. The dimensions of battery are illustrated in Figure 4.1. These batteries are hermetically sealed units with plastic prismatic case with ribs, and are fitted with a safety vent for protection and/or rupture of the cell case. Under normal conditions of use, the solid electrode materials and liquid electrolyte contained are non-reactive and non-explosive (Material Data Sheet (1) 2008). There is no danger if the battery case split caused by strong impact or shock during operation; however, it must be discharged completely and replaced immediately since it happens (Material Data Sheet (1) 2008). The battery may release heat during normal discharging and especially the temperature will rise to 80°C - 100°C if battery is charged and discharged by big current. The temperature durability of the battery case is 250°C (Material Data Sheet (1) 2008).

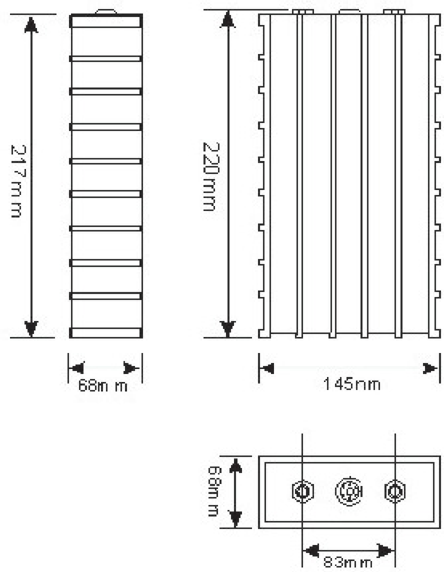

Figure 4.1: Dimensions of the lithium-ion battery

4.1.1.3 ADRs and NCOP

To register the REV vehicle as a standard Australian road vehicle, the modified Hyundai Getz must be compliant to with applicable codes specified in the ADRs and the NCOP, Section LO. Hyundai Getz is classified as a passenger vehicle and has a vehicle category code of MA. In this section the codes and regulations that are relevant to the battery compartment design will be discussed.

The NCOP states that the batteries must be fixed in position and will not easily break in a crash. The battery restraint system must adequately withstand four various impact conditions, which are 20-g frontal impact, 15-g side impact, 10-g rear impact and 10-g vertical impact conditions. Besides, the tyre and axle loadings of the converted vehicle must not be overloaded due to the increase in weight caused by the addition of the batteries.

In addition, batteries that contain liquid or evolve gases must be either fully enclosed in a sealed compartment or individually sealed and externally vented. The battery compartment must be either constructed of or coated with a durable corrosion resistant material that does not shrink or crack under the vibrations and temperatures likely to be encountered in a motor vehicle. Furthermore, the battery compartment must be labelled with the appropriate hazard symbols and indicative voltage likely to be encountered as chemicals contained in the batteries may cause hazard in the event of a crash (Australian Motor Vehicle Certification Board Working Party 2006).

A forced ventilation system might be required if gases are given off by the batteries during normal battery operation. The ventilation system must be corrosion resistant and adequately protected from mechanical damage, and designed in such a way that it will not ignite the vented gases. Moreover, the air inlet and outlet of the ventilation system must be located at opposite ends of the battery compartment (Australian Motor Vehicle Certification Board Working Party 2006).

4.1.2 Computer Aided Drafting Modelling

For the virtual prototype of the battery compartment, SolidWorks software, which is a three-dimensional mechanical computer-aided design program, was chosen for its ease, and the ability to build welded structures with custom defined structural members and to allow quick geometric changes.

4.1.2.1 Basic Procedure

The basic procedure for the design of the battery compartment using SolidWorks are as follows:

- A 3D sketch of the battery compartment frame with fully defined dimensions was created

- The battery compartment frame was then created using the custom defined structural members, such as 25 mm x 25 mm x 3 mm angle bar and 32 mm x 13 mm x 1.6 mm rectangular hollow tube

- Parts, such as the reinforcing strap and tube, were designed and modelled

- Parts were then assembled together with the battery compartment frame by creating geometric relationships between assembly components. These geometric relationships included concentric, coincident and distance relationships

- Holes were then created within assemblies using the Hole Wizard in SolidWorks. The Hole wizard allows inserting the right type of hole based on the selected fastener

- Smart Fastener in SolidWorks was then used to inserts fasteners to all holes in the assembly

4.1.3 Finite Element Analysis

With the battery compartment assembly geometry created, an investigation into the stress and strain for the given impact conditions specified in the NCOP was possible with the aid of ANSYS Workbench software. The ANSYS Workbench software was selected for its ease of use and ability to read SolidWorks CAD geometry with no translations and no middle geometry formats.

4.1.3.1 Basic Assumption

For the purpose of this study, four assumptions were made to simplify the analysis of the battery compartment. These basic assumptions are:

- The impact force resulting from the corresponding impact condition was evenly distributed across the corresponding face of the battery compartment frame.

- Only total deformation and safety factor based on the material tensile yield strength will be included in the analysis results as these would be sufficient to determine the potential of failure under specific impact condition.

- The material strength of the battery compartment frame were assumed to be identical to its nominal value

4.1.3.2 Material Property Input

For the finite element modelling, the material properties are tabulated in the following tables

Property	Structural Steel
Yound's modulus (E)	200 GPa (Wikipedia (c) 2008)
Yield Stength	320 MPa (Wikipedia (c) 2008)
Ultimate Strength	460 MPa (Wikipedia (c) 2008)

Table 4.1: Material properties for structural steel

Property	High Tensile Steel
Yound's modulus (E)	200 GPa (Wikipedia (c) 2008)
Yield Stength	634 MPa (Salmon, Johnson & Malhas 2008)
Ultimate Strength	827 MPa (Salmon, Johnson & Malhas 2008)

Table 4.2: Material properties for high tensile steel

4.1.3.2 Basic Procedure

The basic procedure for the finite element analysis of the battery compartment using ANSYS Workbench is as follow:

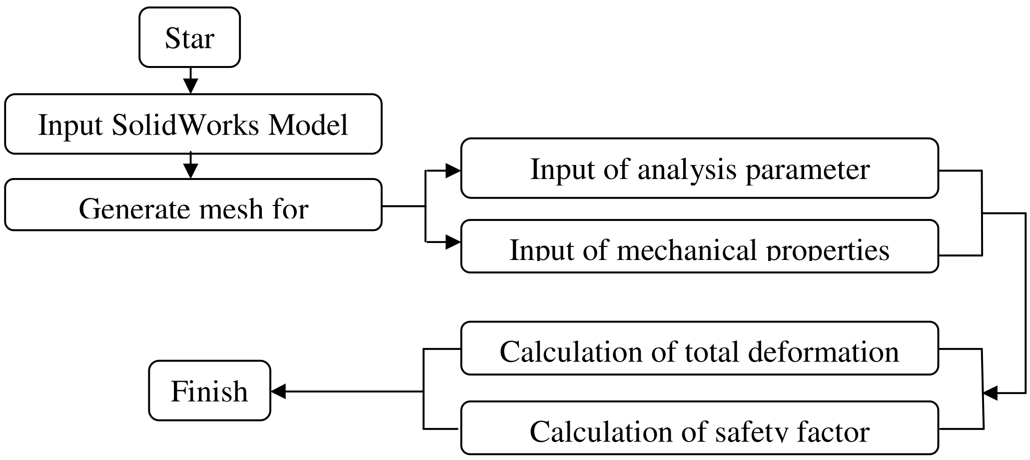

Figure 4.2: The flow of the finite element analysis of the battery compartment frame

4.1.4 *Overview of the Design Process*

The battery restraint system design was an iterative process. The overall design process (see Figure 4.3) was composed of four phases - specification development and planning, conceptual design, detailed design and construction. These phases were the major concerns during the design of the battery restraint system.

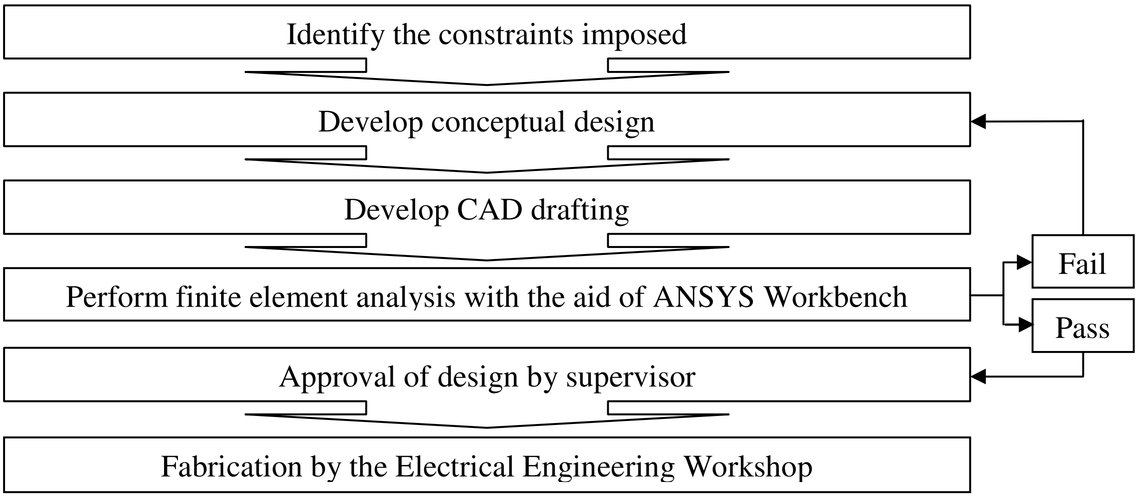

Figure 4.3: Iterative design process for the battery compartment

4.1.4.1 *Specification Development and Planning*

The goals of the specification development and planning phase were to understand the design problem and plan for the design project. Understanding the design problem involved determining the aims of the design project, identifying the relevant codes and regulations that must be adhered to, and setting engineering targets for the design. Once the design problem was completely analysed, a project plan was established for executing the remainder of the design process. The project plan was used for defining the tasks that need to be complete during the design process and provides a clear strategy for proceeding the remainder of the design process.

4.1.4.2 *Concept Design*

During this phase, rough idea was developed and represented by rough sketches and notes. Subsequently, evaluation of the conceptual designs generated was performed based on feasibility judgement, and design specifications and constraints.

4.1.4.3 Detail Design

In this stage the chosen conceptual design was refined into detailed design with all the dimensions and then analysed with the aid of computer softwares. This refinement involved the generation of virtual prototype of the chosen concept design using SolidWorks software. Subsequently, investigation into the stress and strain under specified conditions was conducted using ANSYS Workbench software.

4.1.4.4 Construction

In this stage the finalised design drawing was submitted to the Electrical Engineering Workshop for fabrication if the detailed design was fully evaluated and approval for the construction of the proposed design was granted.

4.2 Results and Discussion

4.2.1 Battery Restraint System Location

For the Hyundai Getz, there were only two options for the battery placement. These included the front engine compartment and rear luggage compartment as illustrated in Figure 4.4 & 4.5 respectively. To determine which location was more desirable for battery placement, both the engine compartment and rear cargo area were analysed based on the available space with the aid of cardboard mock-ups. In the end the rear luggage compartment was chosen as the battery compartment location because it has sufficient space for all the batteries arranging in a single layer as illustrated in Figure 4.6. With this battery arrangement, better accessibility for servicing in future can be obtained. The engine compartment was considered undesirable because it had insufficient space for all the batteries without stacking on top of each other. If the batteries are stacked up, the batteries would not be accessed easily for the installation of wiring and inspection.

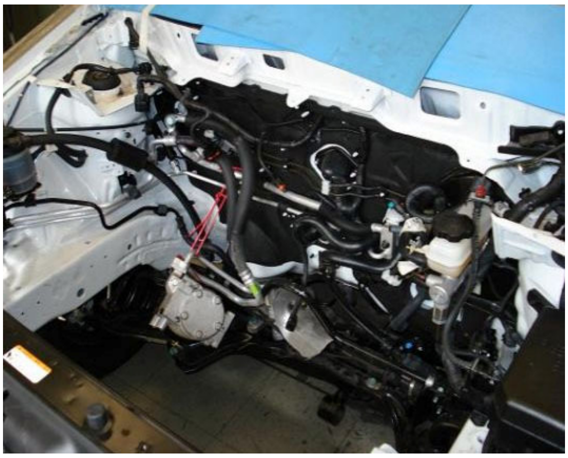

Figure 4.4: Engine compartment after the removal of the internal combustion engine and transmission

Figure 4.5: Rear luggage compartment

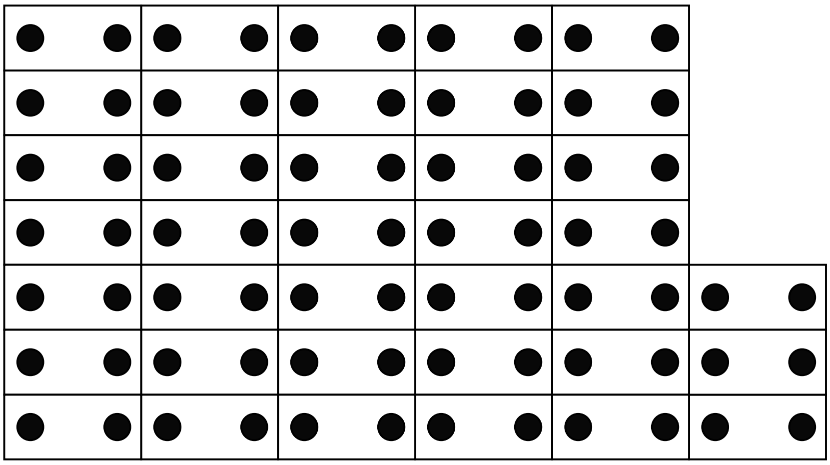

Figure 4.6: Schematic Battery Layout

4.2.2 Battery Compartment Frame Design

The obvious consideration for the design of battery compartment was secure mounting of the batteries even during a collision or rollover. The battery rack must adequately withstand the specified crash accelerations as mentioned in Chapter 5.1.1.3. From this point each progressive design step remained based around this requirement. A brief summary of its conception is as follows.

4.2.2.1 Initial proposal

Figure 4.7 shows the initial proposal for the battery compartment frame. It was basically an attempt to conceptualise the geometry of battery compartment frame. It was proposed to be made of equal angle bar and purposely designed slightly oversized to accommodate battery expansion with use. Besides, extra space was given between the top of battery and the top of rack for the installation of electric vehicle components later. In addition, straps were intended to be fastened to the protruding angle bars across the top with a set of screws and nuts in order to provide vertical protection. These protruding angle bars were intended to be welded onto the side of the frame. Moreover, reinforcing straps were evenly distributed across the bottom to support the batteries weight. Furthermore, the battery charger was intended to be mounted onto the battery compartment frame.

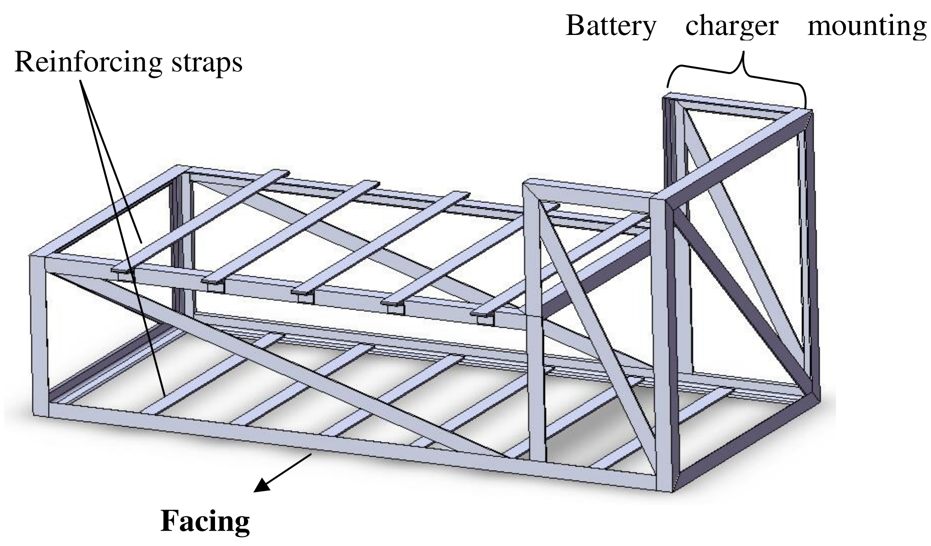

Figure 4.7: Initial proposal for the battery mounting frame

However, the initial design was rejected as it required complicated manufacture because of its inherent three-dimensional geometry. Due to its relatively large size and high degree of shape complexity, the initial proposed design contained many components that must be using welding. As a result of the possible harmful metallurgical effects caused by the welding processes, battery compartment reliability could possibly reduced due to increased possibility of welding part failure. Hence, the initial proposal was rejected for safety reason.

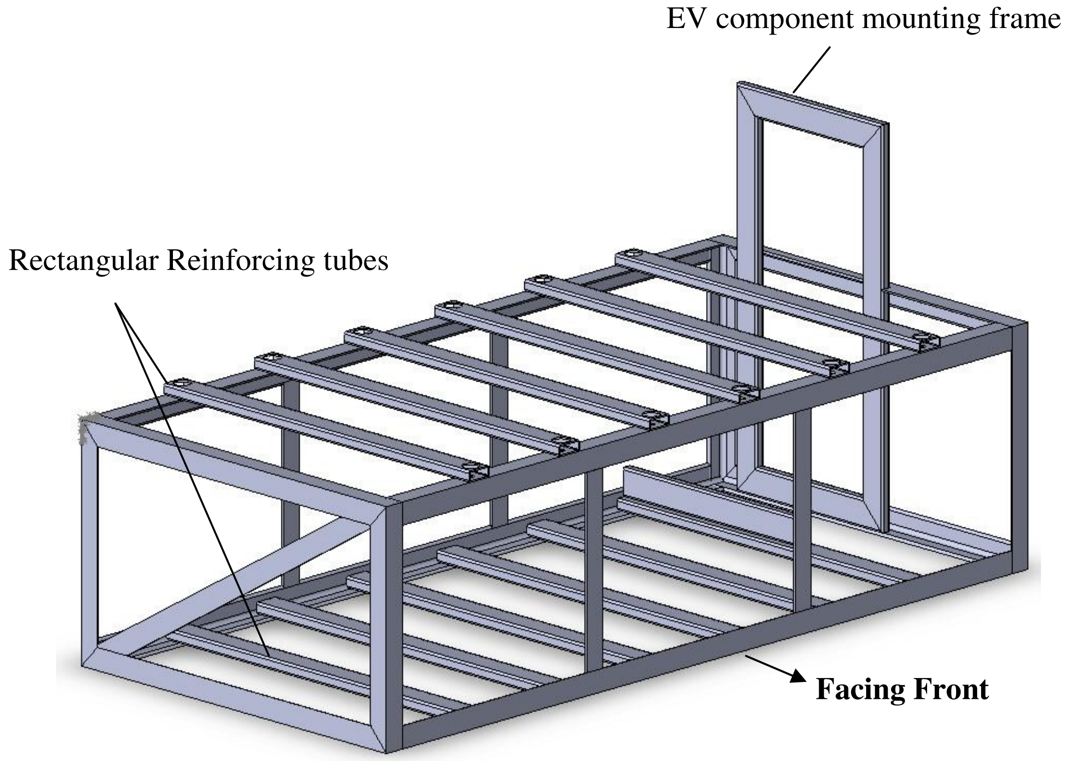

Figure 4.8: Final proposal for the battery compartment frame

4.2.2.2 Final Design

Figure 4.8 shows the final design of the battery compartment frame. The final design contained fewer components that were welded assemblies than the previous idea. The rectangular battery charger component mounting frame in the initial design was replaced with a simpler mounting frame as illustrated in Figure 4.8. These improvements involved less welding processes required and therefore resulted in improved reliability due to reduced possibility of welding part failure. Besides, the rear cargo capacity was increased as a result of the removal of the previous battery charger mounting frame. In addition, the straps across the top and bottom proposed in the initial design were swapped with rectangular bars for further reinforcement. The bars across the bottom were intended to be welded onto the battery compartment frame whereas the bars across the top were intended to be directly fastened to the frame with a set of screws and nuts. Furthermore, cylindrical blocks as illustrated in Figure B.2 were intended to be fastened to the top reinforcing bars in order to hold the batteries down. These blocks were made from plastic cylindrical blocks to avoid accidental short across two terminals and were located at the corners of the batteries to avoid interference with the copper strap interconnected across the batteries. Moreover, the battery compartment was intended to be mounted onto the chassis of the vehicle with four 8 mm bolts, located at the bottom corners of frame.

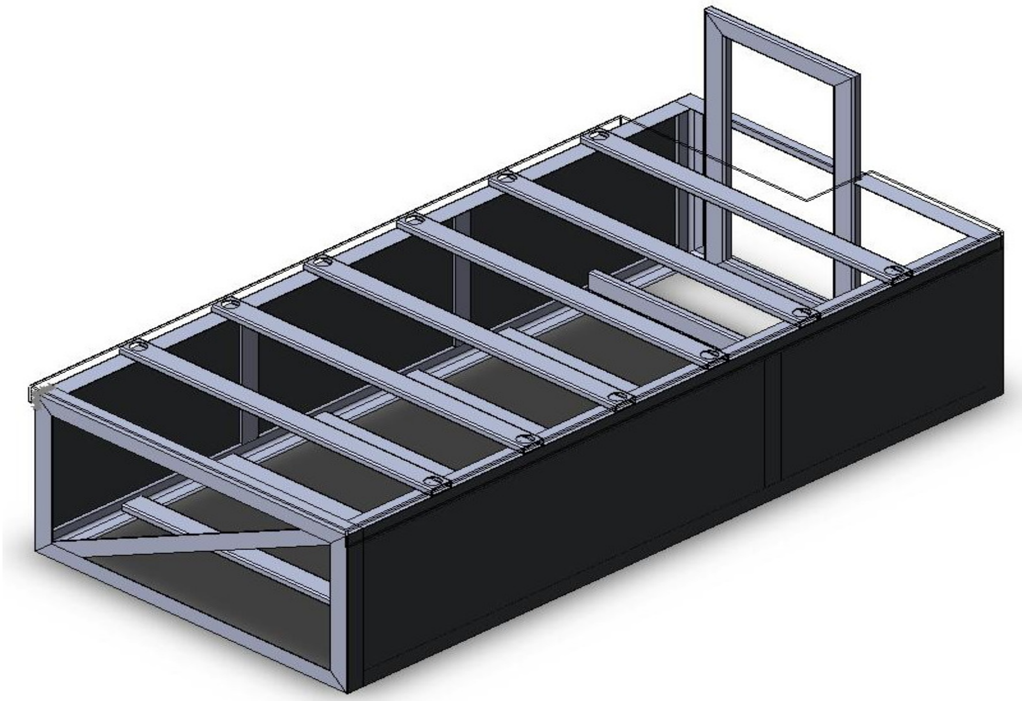

Figure 4.9: Final battery compartment proposal

Figure 4.9 shows the finalised battery compartment. The battery compartment was partially enclosed with a transparent plastic cover placed on top and two metal plates bolted onto the front and rear ends while left and right sides were uncovered. There were four main reasons for this arrangement. Firstly, the plates and cover could prevent things from falling into the battery compartment. Besides, both the batteries and the passengers could be protected in an accident with the front and rear covers mounted. In addition, the transparent cover allows easy inspection of the batteries without disassembly of the top reinforcing bars. Furthermore, heat generated by the batteries during operation and charging could be released to the surrounding from the sides. Moreover, it was proposed that labels with the appropriate hazard symbols and indicative voltage likely to be encountered would be placed on top of the transparent plate as shown in Figure B.1.

4.2.3 Material Selection

For the battery compartment, it was first proposed to be fabricated with aluminium alloy as aluminium alloy is lighter and more corrosion than steel. However, the aluminium alloy angle stock and rectangular stock have relatively lower ultimate tensile strength and yield strength than the steel. Thus, steel angle stock and rectangular stock were chosen instead. The final design of the battery compartment frame was fabricated with steel equal angle stock with a dimension of 25 mm wide and 3 mm thick while the reinforcing tubes were steel rectangular stock with a dimension of 32 mm wide, 13 mm height and 1.6 mm thick.

4.2.4 Finite Element Analysis of the Final Battery Compartment Design

With the CAD model established, stress and strain analyses of the battery compartment under specified crash conditions were conducted on the battery compartment. In order to ensure that the battery compartment withstand the crash conditions specified in the NCOP, total deformation and safety factor contours were taken for each of the specified impact conditions. These plots provided the information about the physical deformations and safety factors based on the tensile yield strength.

4.2.4.1 Front Impact

After the finite element analysis, the maximum deflection and minimum safety factor could be predicted. They are shown in Figure 4.10 and 4.11 respectively. From the analysis results, the battery compartment frame performed reasonably well under the 20g front impact condition, which is equivalent to 28512N impact force. The maximum total deformation was found to be 2.12 mm occurred at the top centre of the battery compartment frame, with the safety factor greater 1. The minimum safety factor of the assemblage was found to be 1.0086 located the corner as shown in Figure 4.11. This indicates that the battery compartment frame could be strong enough to withstand the front impact force of 28152 N applying on the front end.

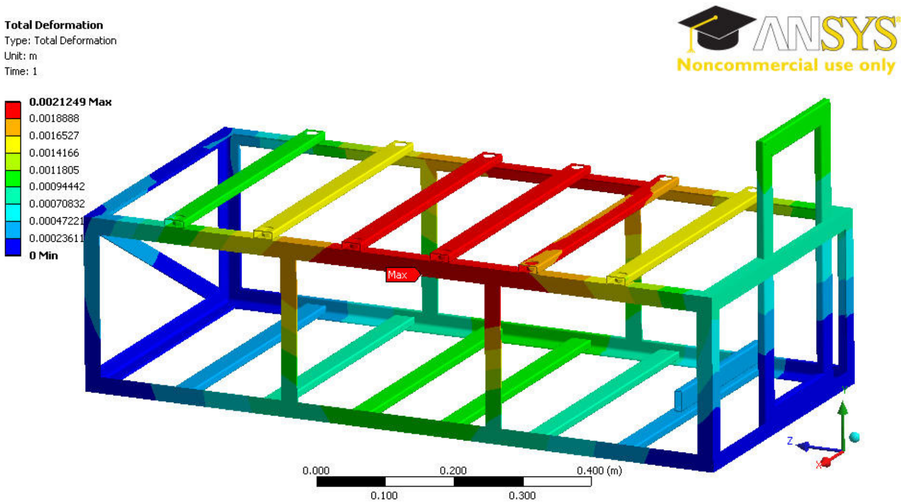

Figure 4.10: Total deformation contours (Front Impact)

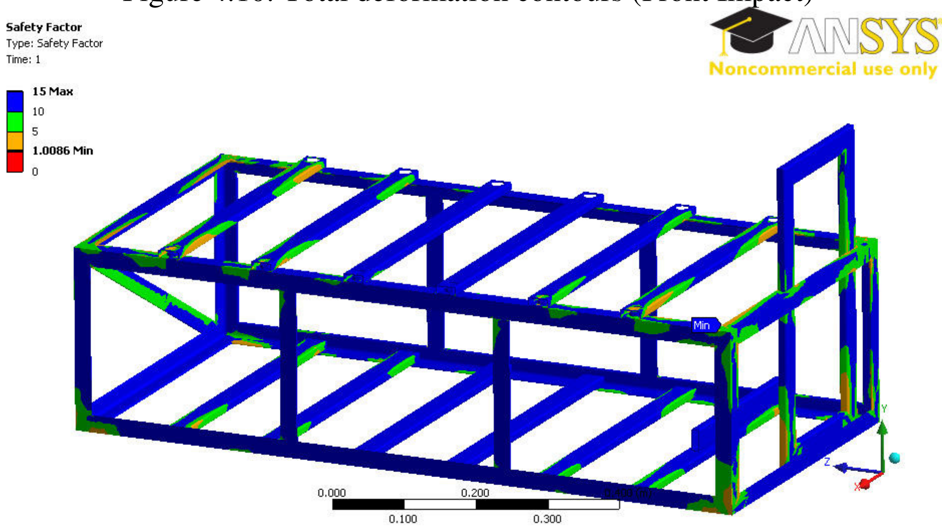

Figure 4.11: Safety factor contours (Front Impact)

4.2.4.2 Rear Impact

The total deformation and safety factor of the battery compartment frame were obtained after the finite element analysis. They are shown in Figure 4.12 and 4.13. The analysis results show that the battery compartment frame is safe as the minimum safety factor of the frame is 1.6073. The maximum deformation was found to be 1.28 mm located at top centre part of the compartment frame.

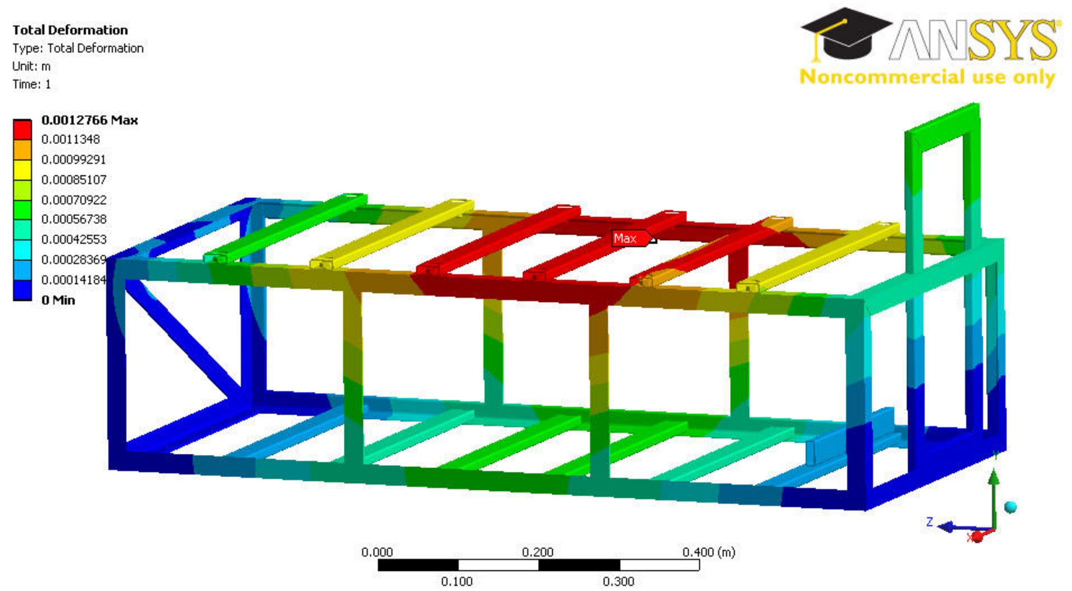

Figure 4.12: Total deformation contours (Rear Impact)

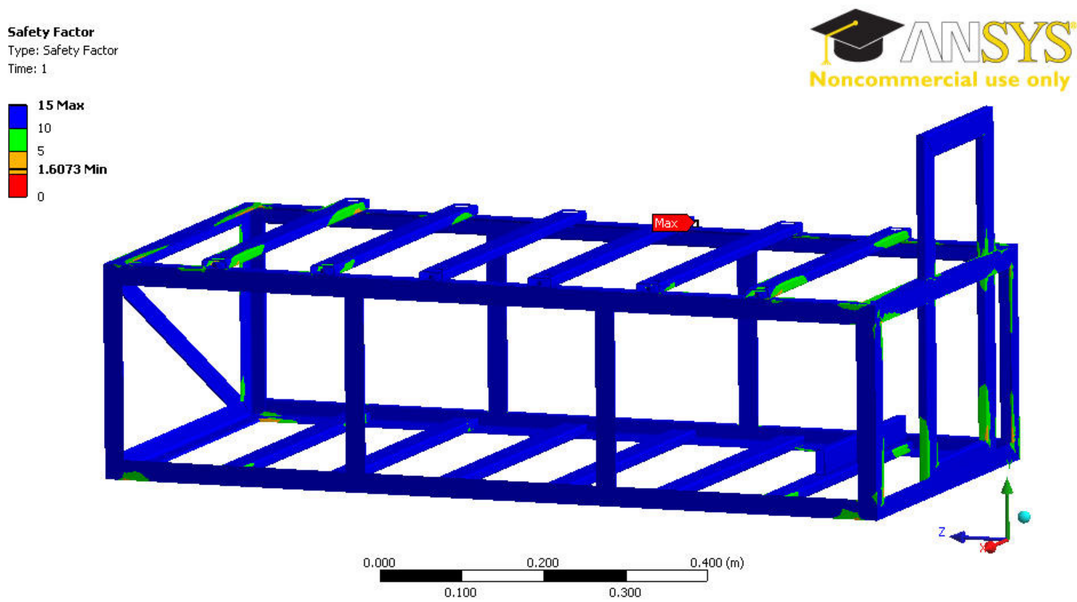

Figure 4.13: Safety factor contours (Rear Impact)

4.2.4.3 Left Side Impact

The finite element analysis results of the compartment frame under 15 g left-side impact condition are shown in Figure 4.14 and 4.15. The results show that the battery frame could withstand the left-side impact without failure with a minimum safety factor of 1.3082. The maximum deformation under left-side impact was found to be 3.443 mm located at the corner of the battery charger mounting frame as shown in Figure 4.14.

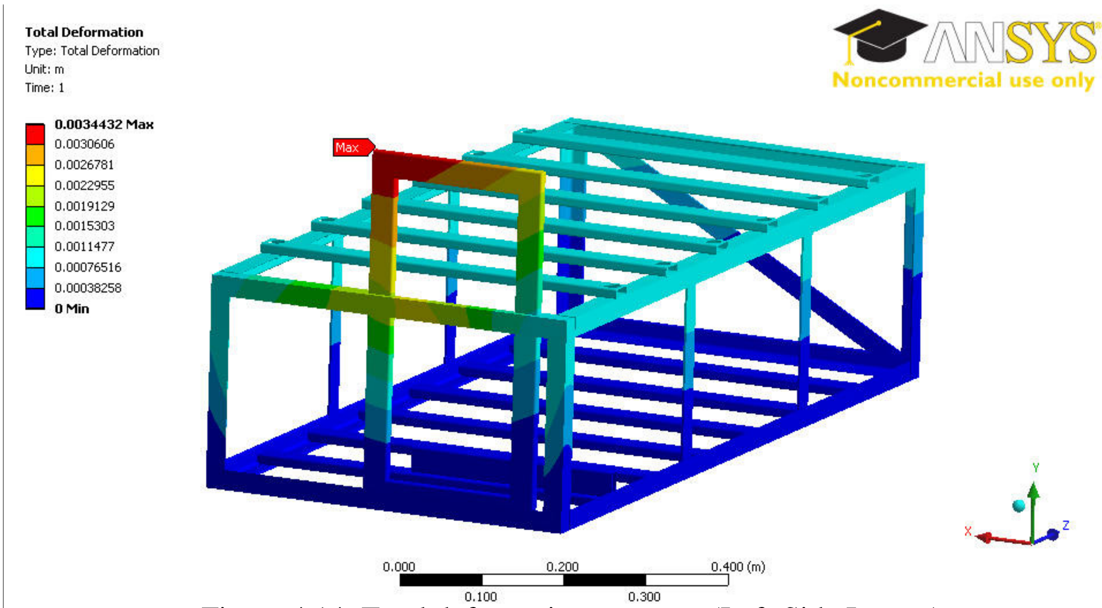

Figure 4.14: Total deformation contours (Left-Side Impact)

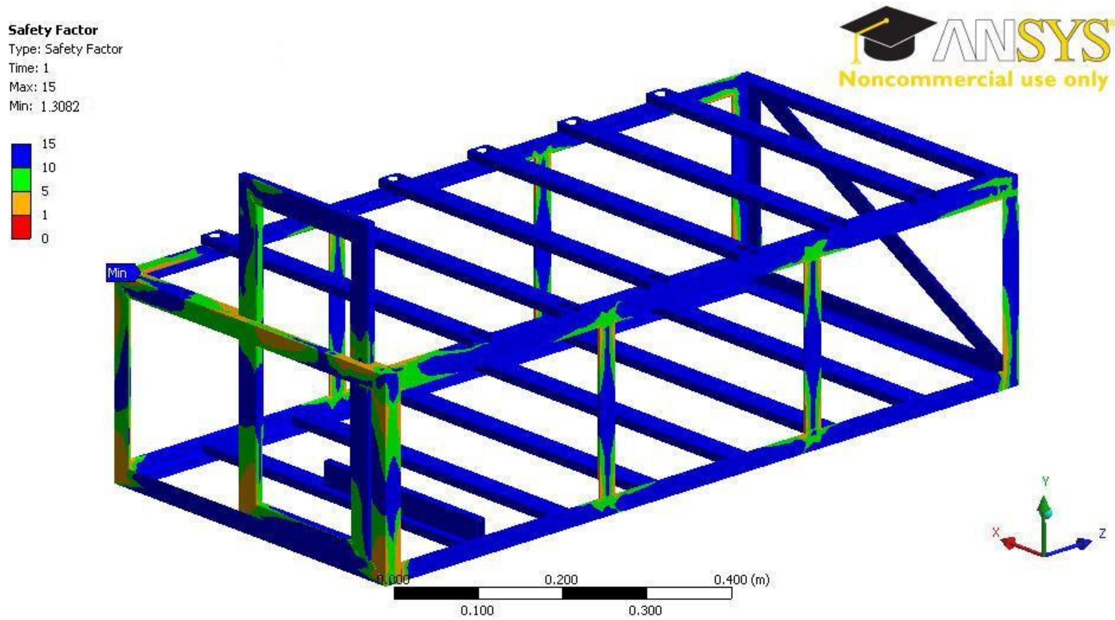

Figure 4.15: Safety factor contours (Left-Side Impact)

4.2.4.4 Right Side Impact

From the analysis results as shown in Figure 4.16 and 4.17, the battery compartment frame performed reasonably well under 15 g right-side impact. The minimum assembly's safety factor was found to be 1.26093 located at upper left-hand corner as shown in Figure 4.17. The maximum deformation of the compartment frame occurred at the upper centre part of the right-side frame with a magnitude of 3.312 mm.

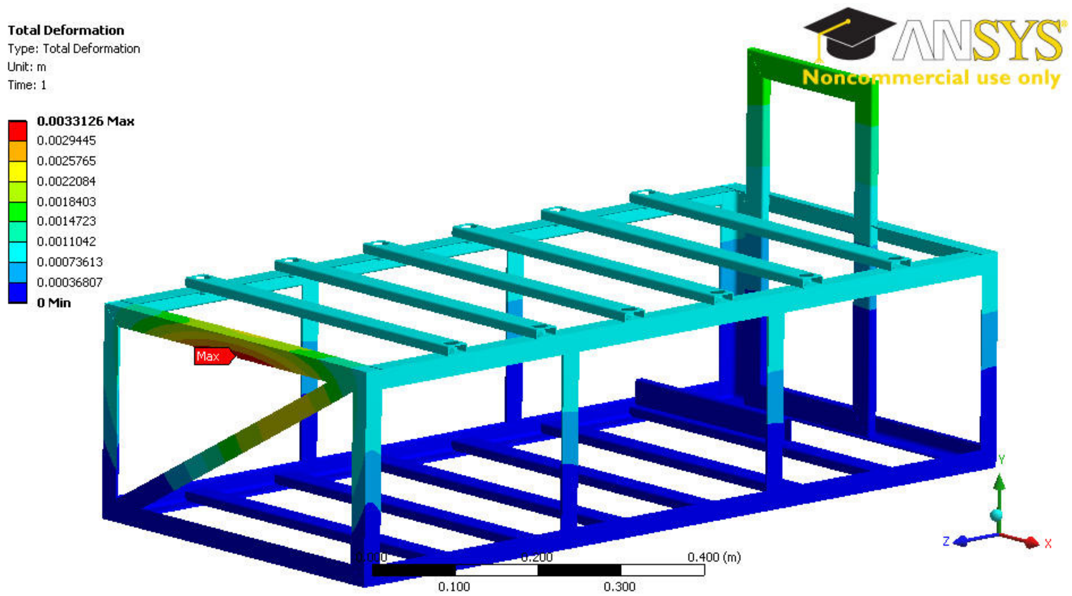

Figure 4.16: Total deformation contours (Right-Side Impact)

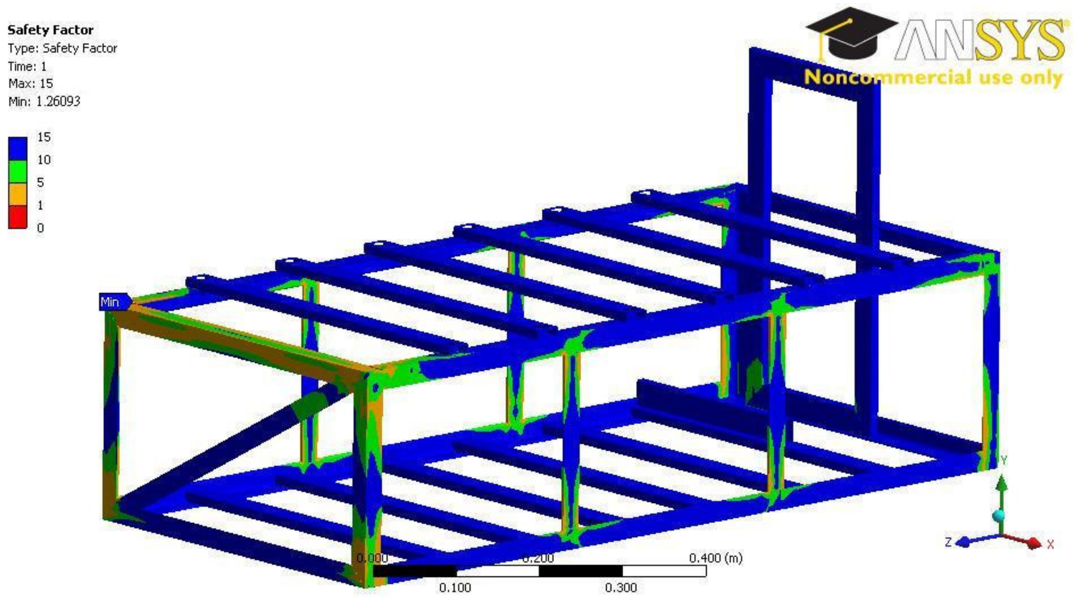

Figure 4.17: Safety factor contours (Right-Side Impact)

4.2.4.5 *Vertical Impact*

The analysis results under 10 g vertical impact were satisfactory. The total deformation and safety factor contours are shown in Figure 4.18 and 4.19 respectively. Although the results show that the reinforcing tubes across the top were subjected to high tensile stress, the maximum deformation among the tubes was found to be 5.024 mm with a minimum safety factor of 1.2087. For this reason, the author believed that the compartment frame could be safe under 14126 N vertical impact force.

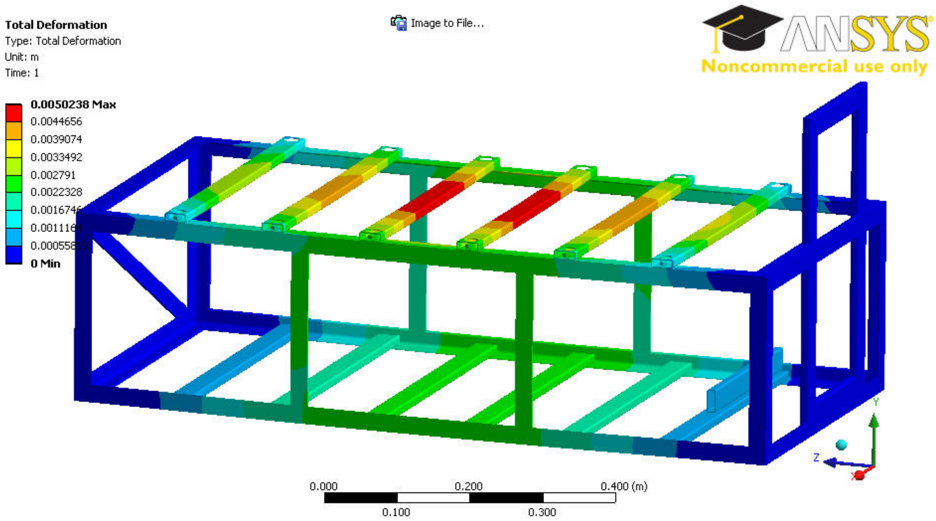

Figure 4.18: Total deformation contours (Vertical Impact)

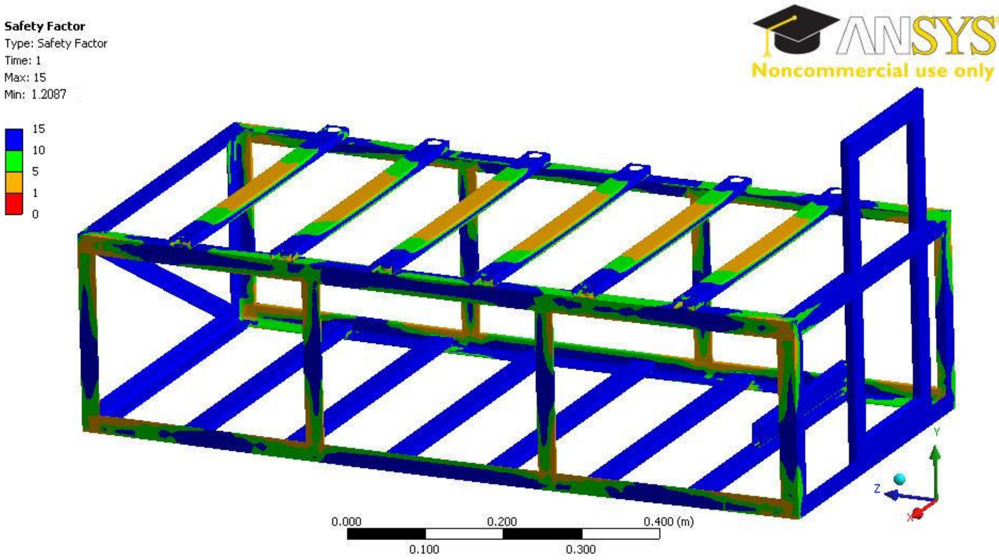

Figure 4.19: Safety factor contours (Vertical Impact)

4.2.4.6 Summary

In summary, the finite element analysis was used to testify whether the compartment frame design would be safe if it is subjected to the impact forces specified in the NCOP. The analysis results were satisfactory as the results indicate that the compartment frame could withstand the corresponding impact conditions with a minimum safety factor greater than 1 for each particular situation.

4.2.6 Limitations of Finite Element Analysis

The finite element analysis of the battery compartment had a limit placed on the simplifying assumptions. This meant that a complete analysis of very high accuracy could not be obtained. The accuracy of the model greatly depended upon material strength of the battery compartment frame. As a result of the heating and cooling of the welding process, the structure of the metal compartment frame may be significantly altered (Degarmo, Black & Kohser 2003). The accuracy of the analysis results could be done better by increasing the level of mesh refinement.

4.2.7 Manufacture

The final design of the battery compartment was submitted to the Electrical Engineering workshop for fabrication after approval of construction was granted from the supervisor. The final product was fabricated with steel equal angle stock with a dimension of 25 mm wide and 3 mm thick while the reinforcing tubes were steel rectangular stock with a dimension of 32 mm wide, 13 mm height and 1.6 mm thick. The steel rectangular tubes and steel angle stock were first cut into shorter individual parts. Then the assembly of the major battery compartment frame including the reinforcing tubes across the bottom was welded by MIG welding technique. The plastic hold-down blocks were fastened to the bottom of the reinforcing tubes with a set 8 mm high tensile bolts and nuts. In addition, the reinforcing tubes across the top were bolted onto the top of the battery compartment frame using 8 mm bolts and nuts. Besides, the compartment frame was bolted onto the chassis of the Hyundai Getz using four sets of 8 mm high tensile steel bolt and nut, locating at the corner inside the compartment frame. Moreover, the aluminium plates located at the front and rear sides were riveted together with the compartment frame.

5 Ride Height and Weight Distribution Evaluation of Hyundai Getz

5.1 Introduction

For a road vehicle, suspension system is used to isolate the vehicle itself and cargo or luggage from severe levels of shock and vibration induced by the road surface. Ride height and front to rear weight distribution are the critical factors that govern several characteristics of a vehicle. For most typical electric vehicle conversion, the original front to rear weight distribution would possibly be altered due to the addition mass gained and removal of some of the internal combustion engine components. Consequently, ride height would be gained or lost. Alteration in the weight distribution and ride height would probably cause handling problems. Therefore, it was crucial to evaluate the ride height, and the front to rear weight distribution of the converted Hyundai Getz and compare the results using a standard Hyundai Getz as a datum.

5.2 Methodology

5.2.1 Ride Height Measurement

To measure the ride height of the converted Hyundai Getz, all measurements were made vertically with the vehicle on a flat, level surface and were made between the wheel centre and top of the wheel arch opening as illustrated in Figure 5.1. Besides, all unusual amounts of weight were removed from the interior of the car. In addition, measurements were made under several different conditions in order to determine the variations in ride height between the maximum and minimum laden sprung masses of the car. These conditions included vertical measurements at un-laden mass, and in two-occupant, four-occupant and five-occupant conditions.

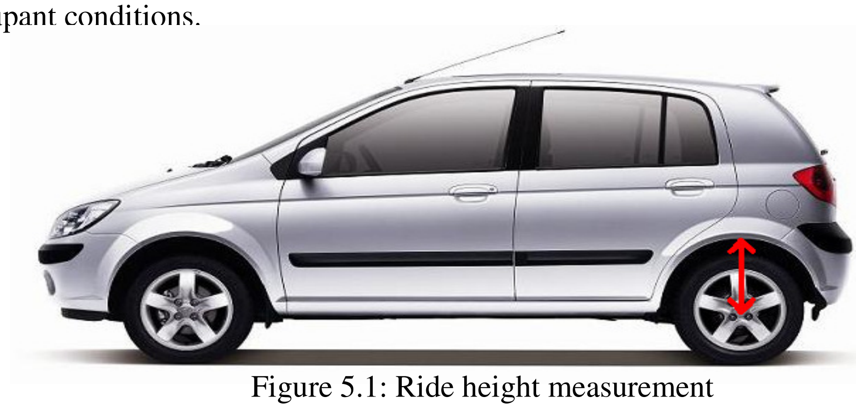

Figure 5.1: Ride height measurement

5.2.2 *Front-to-Rear Weight Distribution Calculation*

5.2.2.1 *Basic Assumptions*

For the calculation of the front-to-rear weight distribution, four assumptions were made to simplify the calculation. These basic assumptions are:

- Only the major components that are the dominant contributors to the curb weight were taken into account. These components included the electric motor, fuel tank, batteries and the battery compartment frame.
- The centres of gravity of all the components were assumed to be acting along the longitudinal centreline which is 3825 mm long.
- The calculation of the height of the centre of gravity was not conducted as it is not related to the front-to-rear weight distribution calculation.
- The original front-to-rear weight distribution of the Hyundai Getz is 63:37 (Cartoday 2006).

5.2.2.2 *Numerical Analysis of the Front-to-Rear Weight Distribution*

To determine the total reaction forces, reaction forces, R_A and R_B, caused by each component added to or removed from the Getz was calculated separately. Figure 5.2 was used for the determination of the front-to-rear weight distribution.

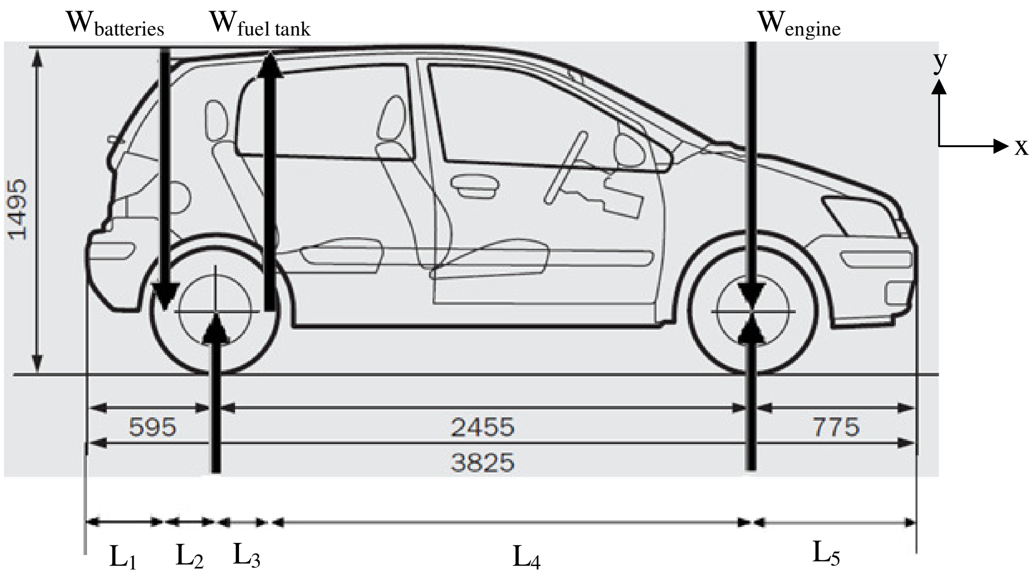

Figure 5.2: Schematic diagram of the Hyundai Getz

Some important definitions for the numerical analysis of the converted Hyundai Getz front-to-rear weight distribution are listed below:

Component	Weight (kg)
Original combustion engine	68.6
Electric motor	133.4
Fuel tank with 45 L of gasoline	48.74
Batteries including the battery compartment	151

Table 5.1: Component weight of the converted Hyundai Getz

By applying Newton's third law and using static equilibrium position, the reaction forces at the front and rear axles can be formulated.

1st Step - Consider only W_{engine} is acting on the car,

$$\sum M_A = 0 \tag{5.1}$$

$$(L_3 + L_4) \times W_{engine} = (L_3 + L_4) \times L_{B1} \tag{5.2}$$

and

$$\sum F_y = 0 \tag{5.3}$$

$$R_{A1} = W_{engine} - R_{B1} \tag{5.4}$$

where W_{engine} is weight of electric motor minus the weight of the combustion engine.

2nd Step - Consider only $W_{fuel\ tank}$ is acting on the car,

$$\sum M_A = 0 \tag{5.1}$$

$$L_3 \times W_{fuel\ tank} + (L_3 + L_4) \times R_{B2} = 0 \tag{5.5}$$

and

$$\sum F_y = 0 \tag{5.3}$$

$$R_{A2} = -W_{\text{fuel tank}} - R_{B2} \tag{5.6}$$

where $W_{\text{fuel tank}}$ is the weight of the fuel tank including 45L of gasoline.

3rd Step - Consider only $W_{\text{batteries}}$ is acting on the car,

$$\sum M_A = 0 \tag{5.1}$$

$$L_2 \times W_{\text{batteries}} + (L_3 + L_4) \times R_{B3} = 0 \tag{5.7}$$

and

$$\sum F_x = 0 \tag{5.3}$$

$$R_{A3} = W_{\text{batteries}} - R_{B3} \tag{5.8}$$

4th Step – Solve Equations 5.2 and 5.4 – 5.8, R_A and R_B can be calculated as follow:

$$R_A = R_{A1} + R_{A2} + R_{A3} \tag{5.9}$$

$$R_B = R_{B1} + R_{B2} + R_{B3} \tag{5.10}$$

5th Step – Front and rear weight distribution can be calculated by,

$$\text{Front weight distribution} = \frac{R_B}{R_A+R_B} \tag{5.11}$$

$$\text{Rear weight distribution} = \frac{R_A}{R_A+R_B} \tag{5.12}$$

5.2 Results and Discussion

5.2.1 Ride Height Evaluation

Table 5.1 and 5.2 show the results of the vertical measurement under various conditions for the converted Getz and standard Getz respectively. From the results, it can be seen that ride height decreases as the number of occupant increases.

Condition	Front (mm)	Rear (mm)
Vertical measurement wheel centre to the top of wheel arch opening at un-laden mass	370	330
Vertical measurement wheel centre to the top of wheel arch opening with 2 front-seat occupants	355	320
Vertical measurement wheel centre to the top of wheel arch opening with 2 front-seat occupants and 2 rear-seat occupants	350	310
Vertical measurement wheel centre to the top of wheel arch opening with 2 front-seat occupants and 3 seat-seat occupants	340	300

Table 5.1: Vertical measurement from the wheel centre to the top of wheel arch opening under different conditions (Converted Hyundai Getz)

Condition	Front (mm)	Rear (mm)
Vertical measurement wheel centre to the top of wheel arch opening with 2 front-seat occupants	345	330
Vertical measurement wheel centre to the top of wheel arch opening with 2 front-seat occupants and 2 rear-seat occupants	320	325
Vertical measurement wheel centre to the top of wheel arch opening with 2 front-seat occupants and 3 seat-seat occupants	315	310

Table 5.2: Vertical measurement from the wheel centre to the top of wheel arch opening under different conditions (Standard Hyundai Getz)

From the comparison between the Table 5.1 and 5.2, it could be seen that the front-end of the converted Getz is lifted up whereas rear-end of the converted Getz sits lower than the standard Getz as expected. This could be explained by the addition mass of the batteries added to the rear luggage compartment and the removal of the original internal combustion engine from the front engine compartment.

As a result of increment in the front ride height caused by the removal of the internal combustion engine and the addition mass added by the batteries, the headlamp aiming may also be affected, which in turn affects night-time driving safety as mentioned in Chapter 2.5.1. For this reason, evaluation of the converted Getz headlamp aiming was conducted. It was found that the altered headlamp aiming was raised by 30 mm. In order to maintain good headlamp aiming condition, the headlamp and fog lamp aiming points were adjusted with the guidance of the Hyundai Shop Manual.

Although the difference in ride height between the converted Hyundai Getz and standard Hyundai Getz was relatively small, further investigation into the suspension geometry should be conducted as the alteration in ride height may possibly upset the steering geometry of the front suspension (Carley 2005). The suspension geometries, such as the camber angle, caster angle and king pin angle, should be investigated to determine if the manufacturer specifications are altered.

5.2.2 Weight Distribution Evaluation

The results of the front-to-rear weight distribution are shown in Table 5.3. It can be seen that the load distributed to the front axle was decreased by 8.1 %. This could be explained by two main reasons. One is the removal of the original combustion engine. The other is the addition mass added by the batteries at the rear luggage compartment.

	Front/Rear Weight Distribution (%)
Converted Hyundai Getz	54.9 : 45.1
Standard Hyundai Getz	63 : 37

Table 5.3: Comparison of front/rear weight distribution between the converted and standard Getz

Although the original front-to-rear weight distribution was altered due to the conversion, the new weight distribution was desirable because it offers inherent handling stability during cornering (Bastow, Howard & Whitehead 2004). For a front-heavy car, it tends to travel in straight line and has a relatively small wind-induced yawing moment due to its configuration as mentioned in the literature survey. However, the calculation can only serve as a reference due to its unrealistic assumptions.

For this reason, it is suggested that further investigation into the weight distribution should be conducted. This could be done easily by placing four scale underneath the front and rear tyres. The reason why the author did not conduct this method was that there was no appropriate scale available that would be used to in UWA. However, this could be done by the garage shop at which the professional could conduct the weight distribution measurement. Once the weight distribution is determined, investigation into the effect on handling behaviour could be conducted easily as the author has already established the procedure for the handling behaviour analysis based on the evaluation of front-to-rear weight distribution.

6.0 Conclusion

Below is a critical assessment of the success achieved in completing the project objectives outlined in Section 1.2.

- The literature survey highlighted the importance of ride height and weight distribution on vehicle handling behaviour. The survey also provides some of the design concepts for the battery compartment design that are commonly used in existing electric vehicle

- The investigation of ride height and weight distribution provided an understanding of the effects of variations in ride height and weight. The understanding assisted in the handling behaviour of the converted Hyundai Getz.

- The propulsion power required by the Hyundai Getz was evaluated by calculating the corresponding road forces acting on the vehicle.

- The battery compartment design was compliant with the identified constraints imposed by the relevant rules and regulations and the REV project aims.

- SolidWorks software package was used to develop the prototype for the potential battery compartment frame design.

- The potential designs for the battery compartment frame were analysed under the impact conditions specified in the relevant regulations with the aid of ANSYS Workbench software package.

- The handling behaviour of the converted Hyundai Getz was fully evaluated using a standard Hyundai Getz as datum.

7.0 Recommendations

The successful completion of this project has produced a reliable, robust foundation for further research to take place. Listed below are the key recommendations for future REV battery restraint system design project and performance evaluation project. These recommendations are useful for those who will do research in the same area.

7.1 Battery Restraint System

- The battery restraint system could be further reinforced by increasing the component dimensions. This could reduce the failure probability due to unexpected load condition and unsuspected flaws.

- Evaluation for the material selection should be conducted in order to select a suitable material that offers a greater material strength with reduced density.

- The batteries could be enclosed in a box using 3 mm aluminium plate as both the batteries and passengers in an accident could be protected by the box.

- Analysis of the heat generation of the batteries during operation should be performed to determine if a ventilation system is necessary.

7.2 Handling Behaviour Evaluation

- Analysis of the suspension geometry should be conducted to determine if the original geometry is upset due to the variations in ride height.

- Evaluation of the front-to-rear weight distribution for the converted Hyundai Getz should be performed by the once the road licence is granted.

8.0 References

Australian Motor Vehicle Certification Board Working Party 2006, *NCOP14 Guidelines Electric Drive*, Australian Motor Vehicle Certification Board Working Party, Australia

Bastow, D, Howard, G & Whitehead, JP 2004, *Car suspension and handling*, SAE International, Warrendale.

Brant, B 1994, *Build Your Own Electric Vehicle*, TAB Books, United States.

Brown, MP 1993, *Convert It*, Future Books, United States.

Cartoday (2006), *Hyundai Getz 1,4*, [Online], Available from: <www.cartoday.com/content/magazine/roadtests/pdfs/2006/08/01/Hyundai_Getz1,4.pdf> [2 September 2008].

Carley, L 2005, *Chassis Ride Height*, Available from: <http://www.aa1car.com/library/ride2h.htm> [1 September 2008].

Degarmo EP, Black JT & Kohser RA 2003, *Materials and processes in manufacturing*, Wiley, United States.

Material Data Sheet (1) 2008, Thunder Sky Energy Group Limited. Available from: <http://www.thunder-sky.com/technical_en.asp?id=345&typeid=81&orderby=1> [15 October 2008]

Mathew R 2008, *Welcome to the REV Project*, REV Project, University of Western Australia, Available from: <http://www.therevproject.com/> [14 September 2008]

Salmon CG, Johnson JE & Malhas F 2008, *Steel structures: design and behavior*, Prentice Hall, New Jersey

Wan, M 2000, *Handling*. Available from: <http://www.autozine.org/technical_school/handling/tech_handling_6.htm> [29 September 2008]

Wikipedia (a) (2008), *Understeer*, [Online], Available from: < http://en.wikipedia.org/wiki/Understeer> [10 September 2008]

Wikipedia (b) (2008), *Understeer*, [Online], Available from: < http://en.wikipedia.org/wiki/ Density_of_air> [10 September 2008]

Wikipedia (c) (2008), *Understeer*, [Online], Available from: < http://en.wikipedia.org/wiki/ Structural> [28 July 2008]

APPENDIX A Power and Drag Analysis Spreadsheet for Hyundai Getz

The calculation of the power required for the Hyundai Getz was conducted by entering the values of car parameters, tyre parameter, environmental parameters and environmental conditions.

Car Parameters

Car Drag Coefficient, Cr	0.32	
Equivalent Car Frontal Area, Af	2.49	m^2
Car Mass, kg	1565	Kg
Motor Efficiency	88	%

Tyre Parameter

Rolling Resistance Coefficient, Cr	0.011	(from the tyre manufacturer - at 35 psi and 50 mph)

Environmental Parameters

Density of Fluid, p	1.204	kg/m^3	(at 20 °C)
Gravity, g	9.81	m/s^2	

Environment Conditions

Headwind Speed (km/h)	0	km/h	→	0	m/s
Uphill Incline (Slope), S_0	0		→	0	°

(Slope is **Negative** if the ground is slope down)

The resistance forces acting on the car and power required are tabulated in the following table.

Vehicle Speed (km/h)	Relative Wind Speed m/s	Drag Force N	Roll Resistance Force N	Hill-Climbing Force N	Total Resisting Force N	Traction Power Required kW	Power Required from Motor kW
0	0.0	0.0	168.9	0.0	168.9	0.0	0.0
10	2.8	3.7	168.9	0.0	172.6	0.5	0.5
20	5.6	14.8	168.9	0.0	183.7	1.0	1.2
30	8.3	33.3	168.9	0.0	202.2	1.7	1.9
40	11.1	59.2	168.9	0.0	228.1	2.5	2.9
50	13.9	92.5	168.9	0.0	261.4	3.6	4.1
60	16.7	133.2	168.9	0.0	302.1	5.0	5.7
66	18.3	161.2	168.9	0.0	330.1	6.1	6.9
68	18.9	171.1	168.9	0.0	340.0	6.4	7.3
70	19.4	181.4	168.9	0.0	350.2	6.8	7.7
72	20.0	191.9	168.9	0.0	360.7	7.2	8.2
74	20.6	202.7	168.9	0.0	371.6	7.6	8.7
76	21.1	213.8	168.9	0.0	382.7	8.1	9.2
78	21.7	225.2	168.9	0.0	394.1	8.5	9.7
80	22.2	236.9	168.9	0.0	405.8	9.0	10.2
82	22.8	248.9	168.9	0.0	417.7	9.5	10.8
84	23.3	261.2	168.9	0.0	430.0	10.0	11.4
86	23.9	273.7	168.9	0.0	442.6	10.6	12.0
88	24.4	286.6	168.9	0.0	455.5	11.1	12.7
90	25.0	299.8	168.9	0.0	468.7	11.7	13.3
92	25.6	313.3	168.9	0.0	482.1	12.3	14.0
94	26.1	327.0	168.9	0.0	495.9	12.9	14.7
96	26.7	341.1	168.9	0.0	510.0	13.6	15.5
98	27.2	355.5	168.9	0.0	524.3	14.3	16.2
100	27.8	370.1	168.9	0.0	539.0	15.0	17.0
106	29.4	415.9	168.9	0.0	584.7	17.2	19.6
108	30.0	431.7	168.9	0.0	600.6	18.0	20.5
110	30.6	447.8	168.9	0.0	616.7	18.8	21.4
112	31.1	464.3	168.9	0.0	633.2	19.7	22.4
114	31.7	481.0	168.9	0.0	649.9	20.6	23.4
116	32.2	498.0	168.9	0.0	666.9	21.5	24.4
120	33.3	533.0	168.9	0.0	701.8	23.4	26.6

Table A.1: Propulsion power required for the Hyundai Getz

APPENDIX B Photographs of the Fabricated Battery Restraint System

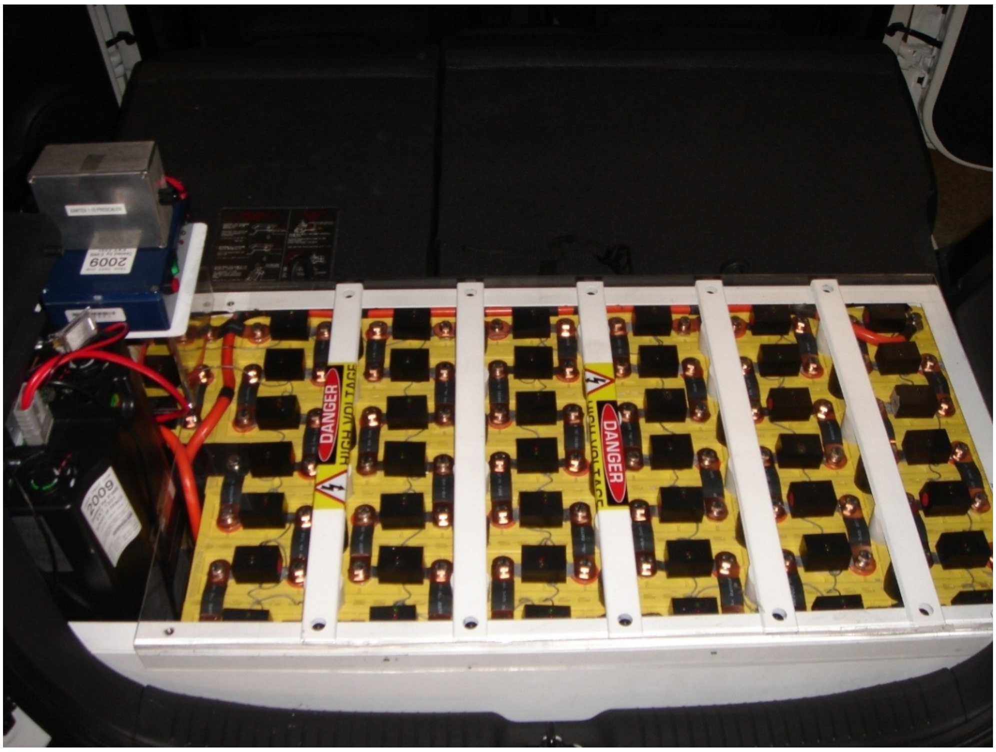

Figure B.1

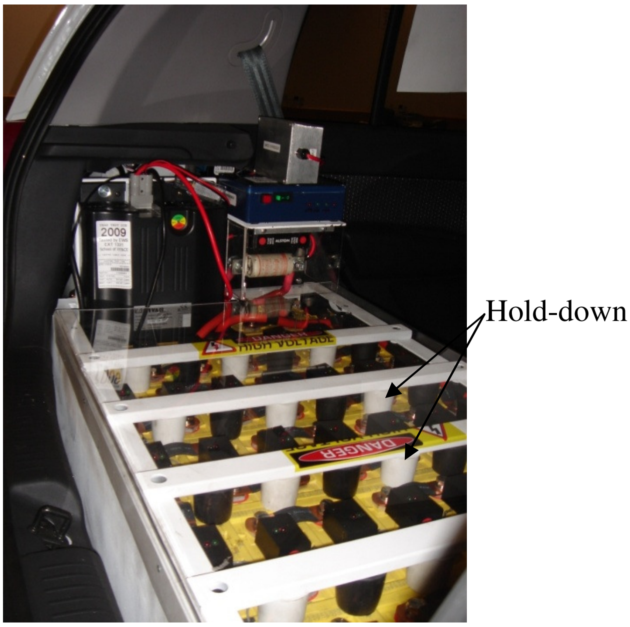

Figure B.2